Simulation of Hybrid Ground Source Heat Pump Systems and Experimental Validation

Jason E. Gentry, jason.earl@okstate.edu
Jeffrey D. Spitler, spitler@okstate.edu
Daniel E. Fisher Ph.D. PE, dfisher@okstate.edu
Xiaowei Xu, xiaowei.xu@okstate.edu

School of Mechanical Engineering
Oklahoma State University
218 Engineering North
Stillwater, OK 74078
USA

ABSTRACT

Hybrid ground source heat pump systems incorporate both ground loop heat exchangers and auxiliary heat rejecters, such as cooling towers, fluid coolers, cooling ponds, or pavement heating systems. The design of the hybrid ground source heat pump system involves many degrees of freedom; e.g. the size of the cooling tower interacts with the control strategy, the ground loop heat exchanger design, and other parameters. This paper presents a simulation of such a system using a direct contact evaporative cooling tower as the supplemental heat rejecter. The simulation is performed in a component-based modeling environment using component models of a vertical ground loop heat exchanger, plate frame heat exchanger, cooling tower, circulating pumps, and heat pumps.

Seven months (March to September 2005) of five-minutely experimental data from a hybrid ground source heat pump system were used for validation purposes. The source side of the system consists of two packaged water-to-water heat pumps, a three-borehole ground loop heat exchanger, and a direct contact evaporative cooling tower, isolated by a plate frame heat exchanger. The load side serves two small buildings with hydronic heating and cooling. Experimental validations of each component simulation and the entire system simulation are presented.

1. INTRODUCTION

Ground source heat pump (GSHP) systems have become increasingly common in residential, commercial, and institutional buildings. In cases where there is significant imbalance between the annual heat rejection to the ground and annual heat extraction from the ground the loop fluid temperature tends to rise (or fall) from year to year. This effect can be moderated by increasing the ground loop heat exchanger size. However, the capital cost requirements can be excessive and an alternative is to add an additional heat sink (or an additional heat source). Systems with additional heat sinks or sources are generally referred to as hybrid GSHP or HGSHP systems.

The most common heat sink device is a cooling tower, but other heat sinks include domestic water heating systems, closed-circuit fluid coolers, ponds, and pavement heating systems. Auxiliary heat sources include solar collectors or boilers.

HGSHP systems seem to have arisen as a practical solution for fixing undersized GSHP systems that have begun to operate too hot (or too cold). The first discussion of design of HGSHP systems for new construction appeared in ASHRAE (1995). For cooling dominated systems, it was suggested that the supplemental heat rejecter could be sized to reject half of the average difference between the heat rejected by the system and the heat to be rejected to the ground for the peak cooling month. The basis for this recommendation is not clear.

Kavanaugh (1998) gives a modified procedure that iteratively approximates the annual heat rejection of the cooling tower or fluid cooler and then recomputes the loop length. The annual heat rejection is estimated using a heuristic expression that gives the equivalent full load run hours for the cooling tower or fluid cooler as a function of the equivalent full load run hours for cooling and the ratio of flow rates between the heat rejecter and the system. An alternative approach is also given which assumes that the heat rejecter can balance the annual heat rejection and heat extraction and then the required run hours for the heat rejecter can be estimated with a heuristic expression.

Several studies have looked at the performance of existing HGSHP systems. Phetteplace and Sullivan (1998) described an HGSHP system with 70 closed-loop boreholes and a 275 kW cooling tower serving a 2,230 m^2 administration building in Louisiana. Singh and Foster (1998) described an HGSHP with 88 boreholes and a 422 kW closed-circuit fluid cooler system serving a 7,436 m^2 office building in Allentown, Pennsylvania.

Yavuzturk and Spitler (2000) described a parametric study of HGSHP system design and control using a system simulation approach. The simulations were developed in the TRNSYS environment, using standard TRNSYS types for the cooling tower, circulating pumps, and controls. The GLHE model (Yavuzturk and Spitler 1999) was based on an extension of past work by Eskilson (1987) to treat short time response. With an open cooling tower, a control strategy which operated the tower when the temperature difference between the exiting heat pump fluid temperature and the wet bulb temperature exceeded a setpoint gave the best results.

Ramamoorthy et al. (2001) reported on a similar study that used a cooling pond as a supplemental heat rejecter. Using a differential temperature control strategy, a limited optimization of GLHE size and pond size was performed.

Chiasson and Yavuzturk (2003) used the same system simulation approach to identify scenarios where an HGSHP system with a supplemental heat source is beneficial, in particular schools in heating-dominated climates, where the school was not operated during the summer. The supplemental heat sources investigated were solar thermal collectors and the approach was shown to be economically feasible.

Khan et al. (2003) described a simulation study of an HGSHP system that utilized a pavement heating system as the supplemental heat rejecter. The approach was similar to the HGSHP studies described above, but was performed within the HVACSIM+ environment.

GSHP systems and GLHE are commonly designed with simulation-based procedures because the long time constant of the ground makes it necessary to ensure that the loop temperatures will not exceed the heat pump limits over the life of the system. Because of the interaction between loop temperatures, GLHE performance, heat pump performance and supplemental heat rejecter performance, simulation is even more needed for design of HGSHP systems.

Never the less, while some validations of GLHE and other HGSHP system components have been reported, no validations of the entire HGSHP system have been reported. Nor, for that matter, have any validations of an entire GSHP system been reported. Several authors have presented validations of ground heat exchanger models – McLain and Martin (1999) and Yavuzturk and Spitler (2001). Thornton, et al. (1997) report on an extensive calibration process which allows a GSHP system simulation to give a good prediction of maximum entering water temperature and heat pump energy consumption compared to the experimental measurements.

While it might be hoped that if each component model of the simulation were validated the entire simulation as a whole would be sufficiently accurate, this is not necessarily the case. In a GSHP or HGSHP system simulation, there is the potential for small errors to accumulate over time. Furthermore, because of the difficulty in characterizing the ground thermal properties, it seems inevitable that, at the least, small errors will always be present. Furthermore, from a designer's perspective, limited information on cooling tower performance, limited accuracy of manufacturer's heat pump data, etc. lead to additional small errors that also may be cumulative. The degree to which this is a problem is unknown, and suggests the need for experimental validation of the entire system simulation. It also suggests the need for experimental validation with and without individual model calibration.

This paper presents an experimental validation of the entire system simulation, using an HGSHP system located at Oklahoma State University. The system size is similar to residential systems, i.e. smaller than a typical HGSHP system. However, it contains all of the components of a typical HGSHP system – a heat pump, three boreholes, and a small direct contact evaporative cooling tower connected via a plate frame heat exchanger. A system schematic is shown below in Figure 1. Furthermore, it is carefully instrumented and monitored, so that the resulting data set is free from significant periods of missing or corrupted data that tend to plague data sets collected with building energy management systems.

The paper is organized by first describing the experimental facility; then the individual component models followed by the overall system simulation approach. This is followed by a comparison between the experimental results and the system simulation results and a discussion of the calibration process which was used to obtain the best match. Finally, the system simulation is reconsidered from the designer's perspective, i.e. if calibration of individual models is impossible, how good are the simulation results that are of primary interest to the designer – energy consumption, cooling tower run time, and peak entering fluid temperature? The accuracy of these results without calibration and with varying degrees of calibration is examined.

2. EXPERIMENTAL FACILITY

The data used to validate the component and system simulations were collected from the HGSHP research facility (Hern 2004) located on the campus of Oklahoma State University. Chilled water and hot water generated with the plant serve two small buildings. The description below is necessarily brief, but a detailed description is given by Hern (2004).

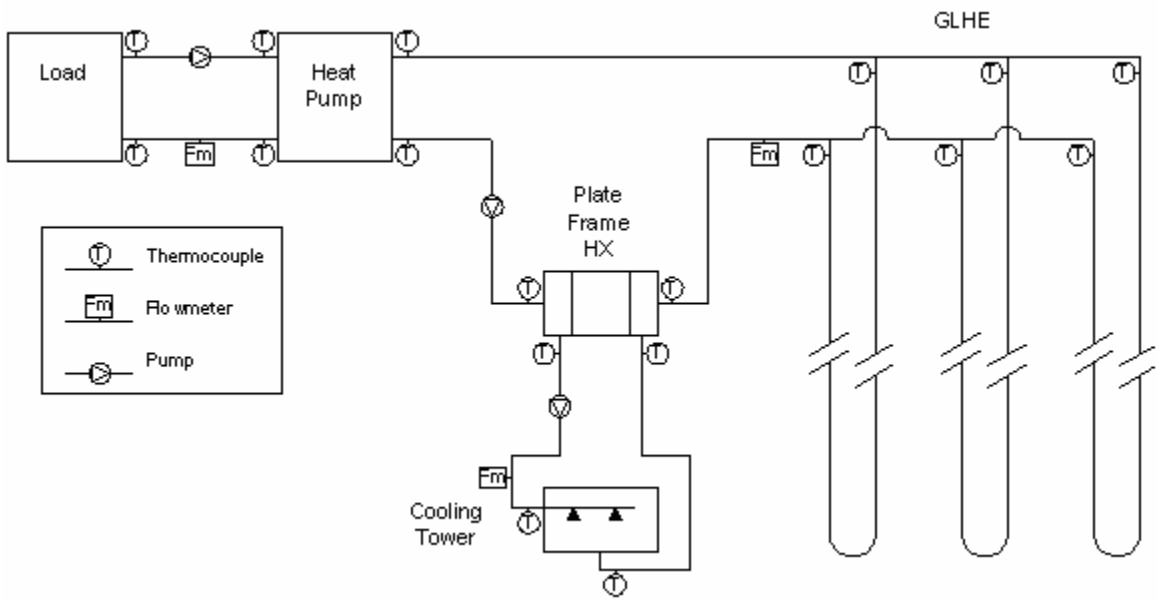

Figure 1. HGSHP configuration for validation

Two identical water-to-water heat pumps, of nominal capacity 10.6 kW are used to provide the chilled water and hot water. For the time period of interest in this simulation, only one heat pump is used at a time. Heating was provided between March 1 and March 29; after which cooling was provided. As the system simulation took the load imposed on the heat pump as a boundary condition, it was possible to model the system with a single heat pump. Catalog data – 35 points in cooling and 25 points in heating mode – at a range of flow rates and entering water temperatures on both the source side and load side are available from the manufacturer and are used to fit coefficients for the model described below.

The facility allows the source side of the heat pumps to be connected to a ground loop heat exchanger, an evaporative cooling tower, and/or a pond loop heat exchanger. These can be connected in any combination, but for the duration of these experiments, they were configured as a typical HGSHP system, with a GLHE, and a cooling tower. The isolation heat exchanger was connected in series with the GLHE, and the cooling tower was switched on and off based on the difference in the exiting heat pump fluid temperature and the outdoor ambient wet-bulb temperature.

The GLHE has, in total, 4 vertical boreholes and one horizontal loop. For these experiments, only 3 vertical boreholes are connected, as shown in Figure 1. The vertical boreholes are each approximately 75 meters deep, 114 mm in diameter and consist of a single HDPE U-tube of

nominal diameter 19.05 mm, backfilled with bentonite grout. The ground thermal conductivity was estimated with an in situ thermal conductivity test (Austin, et al. 2000) and the volumetric specific heat was estimated from knowledge of the geology.

A direct-contact evaporative cooling tower with nominal capacity of 17.6 kW (defined at a water flow rate of 0.63 L/s being cooled from 35ºC to 29.4 ºC with an outdoor wet bulb temperature of 25.6 ºC)is connected to the source-side of the heat pumps via an isolation heat exchanger. No other performance data are available from the manufacturer.

The plate frame heat exchanger has a nominal capacity of 9.3 kW with flow rates of 0.5 L/s on both sides of the heat exchanger and a temperature difference of 19.4°C between the inlet temperatures. The manufacturer gave an additional 15 data points at various flow rates and temperatures.

In addition to the components that are shown explicitly in Figure 1, there is buried piping that connects the GLHE to the plant building (approximately 30 m in each direction), buried piping that connects the cooling tower to the plant building (approximately 31 m in each direction), and exposed (to the plant room environment) piping that connects the components inside the building. Under many conditions, e.g. when the piping is insulated, heat losses and gains to/from the piping may be negligible. However, buried, uninsulated piping, as used to connect the cooling tower and GLHE may have a not-insignificant amount of heat transfer.

A detailed uncertainty analysis was performed by Hern (2004). As can be seen from Figure 1, thermocouples, with an uncertainty of approximately ±0.11°C, were placed on the inlets and outlets of all components. Vortex and paddle wheel flow meters were utilized to measure flow through the heat pump – GLHE loop and through the cooling tower loop; expressions for their uncertainty were given by Hern (2004).

Heat transfer rates are determined as the product of the mass flow rate, specific heat, and ΔT. Given the uncertainty in temperature measurement, the fractional uncertainty in the temperature difference measurement is:

$$e_{\Delta t} = \frac{\pm 0.16^{\circ} C}{\Delta T} \tag{1}$$

Then, the fractional uncertainty of the heat transfer rate may be given as:

$$e_{HTR} = \pm\sqrt{e_{\Delta t}^2 + e_{flow}^2} \tag{2}$$

where e_{flow} = fractional error in the flow rate.

This value changes throughout the experiment for each measurement, but typical values may be given, and for most components, the error bounds on the experimental measurement are also plotted.

3. COMPONENT MODELS

3.1 Heat Pump Model

The heat pump model is a simple water-to-water equation-fit model developed by Tang (2005). The model equations fit power, source side heat transfer rate and load side heat transfer rate to normalized entering fluid temperatures and normalized flow rates. For this application, the model has been recast to take load side heat transfer rate as an input, which is supplied as a boundary condition. The computed load side heat transfer rate and the input load side heat transfer rate are compared and the ratio is used to determine a run time fraction for the time step.

An equation-fit model was initially chosen over a parameter estimation-based model for the relative convenience of determining the inputs and fast execution speed. As was found in the validation, this convenience comes at the cost of poor model performance when one of the input variables falls outside the range of data used to fit the equations.

3.2 GLHE Model

The ground loop heat exchanger (GLHE) model is based partly on the long time g-functions developed by Eskilson (Eskilson 1987) and partly on one-dimensional numerical model used to determine the short time response developed by Xu and Spitler (2006). As the method developed by Eskilson is the basis for the ground loop heat exchanger model, it will be described first. Eskilson's approach to the problem of determining the temperature distribution around a borehole is based on a hybrid model combining analytical and numerical solution techniques. A two-dimensional numerical calculation is made using transient finite-difference equations on a radial-axial coordinate system for a single borehole in homogeneous ground with constant initial and boundary conditions. The thermal capacitance of the individual borehole elements such as the tube wall and the grout are neglected. The temperature fields from a single borehole are superimposed in space to obtain the response from the whole borehole field.

The temperature response of the borehole field is converted to a set of non-dimensional temperature response factors, called g-functions. The g-function allows the calculation of the temperature change at the borehole wall in response to a step heat input for a time step. Once the response of the borehole field to a single step heat pulse is represented with a g-function, the response to any arbitrary heat rejection/extraction function can be determined by devolving the heat rejection/extraction into a series of step functions, and superimposing the response to each step function (Yavuzturk and Spitler 1999). This process is graphically demonstrated in Figure 2 for four months of heat rejection.

The basic heat pulse from zero to Q1 is applied for the entire duration of the four months and is effective as Q1'=Q1. The subsequent pulses are superimposed as Q2'=Q2-Q1 effective for 3 months, Q3'=Q3-Q2 effective for 2 months and finally Q4'=Q4-Q3 effective for 1 month. Thus, the borehole wall temperature at any time can be determined by adding the responses of the four step functions. Mathematically, the superposition gives the borehole wall temperature at the end of the n^{th} time period as:

$$T_{borehole} = T_{ground} + \sum_{i=1}^{n} \frac{(Q_i - Q_{i-1})}{2\pi k} g\left(\frac{t_n - t_{n-1}}{t_s}, \frac{r_b}{H}\right) \quad (3)$$

Where t is the time, s; t_s is the time scale = $H^2/9\alpha$; H is the borehole depth, m; k is the ground thermal conductivity, W/m-K; $T_{borehole}$ is the average borehole temperature in ^oC; T_{ground} is the undisturbed ground temperature in ^oC; Q is the step heat rejection pulse, W/m; r_b is the borehole radius in m; and i is the index to denote the end of a time step (the end of the 1st hour or 2nd month etc.)

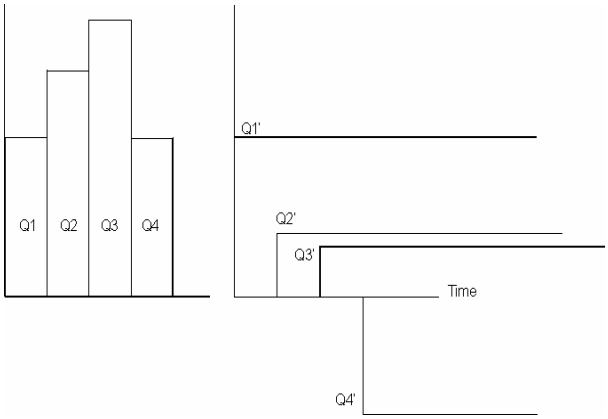

Figure 2. Superposition of Piece-Wise Linear Step Heat Inputs in time (Yavuzturk and Spitler 1999)

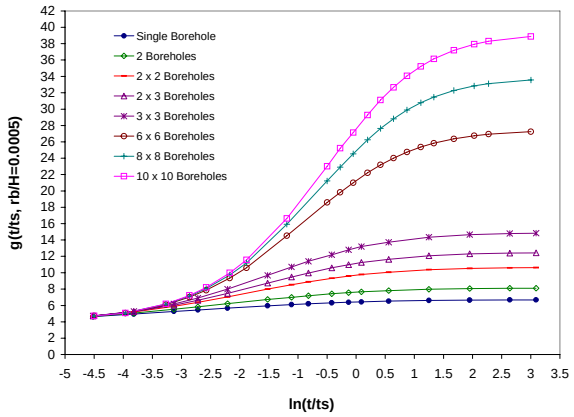

Figure 3. Temperature response factors (g-functions) for various multiple borehole configurations compared to the temperature response curve for a single borehole (Yavuzturk and Spitler 1999)

Figure 3 shows the temperature response factor curves (g-functions) plotted versus non-dimensional time for various borehole configurations with a fixed ratio of 0.1 between the borehole spacing and the borehole depth. The thermal interaction between the boreholes is stronger as the number of boreholes is increased and as the time of operation increases.

The detailed numerical model used in developing the long time-step g-functions approximates the borehole as a line source of finite length, so that the borehole end effects can be considered. The approximation of the borehole as a finite-length line source has the resultant problem that it is only valid for times estimated by Eskilson to be greater than 5 $r^2_{Borehole}/\alpha$. For a typical borehole, that might imply times from 3 to 6 hours. However, much of the data developed by Eskilson does not cover periods of less than a month. (For a heavy, saturated soil and a 76 m deep borehole, the g-function for the single borehole presented in Figure 3 is only applicable for times in excess of 60 days.)

Yavuzturk, et al. (1999) extended Eskilson's long time-step model to short time steps by developing short time-step g-functions with a two-dimensional (radial-angular) finite volume method, which utilized an automated gridding procedure and a "pie-sector" representation of the U-tubes. Because the short time-step g-function represented the response of the entire ground heat exchanger, it necessarily utilized a fixed convective resistance. The authors later found it necessary (Yavuzturk and Spitler 2001) to modify the model to include variable convective

resistance, but this was done at the expense of modeling the thermal mass of the fluid in the borehole.

In order to simultaneously account for variable convective resistance and thermal mass in the borehole, a one-dimensional numerical model is used directly to compute the short time-step response. (Xu and Spitler 2006). This is integrated with Eskilson's long time-step model. By careful control of the one-dimensional model parameters, the model is able to give acceptably accurate short-term response, without the computational time that would be required to run such a model continuously throughout the simulation.

The one-dimensional model has a fluid core, an equivalent convective resistance layer, a tube layer, a grout layer, and is surrounded by the ground. In order to get near-identical results to the more detailed two-dimensional model, it is important to specify the one-dimensional geometry and thermal properties in an "equivalent" manner. This includes conserving the borehole thermal resistance and thermal mass. The model parameters include the number of boreholes, borehole depth and radius, U-tube configurations, the U-tube, the grout and the ground thermal properties, fluid type and fluid factor of the system, and the long time step g-functions. The model is formulated to take inlet temperature and mass flow rate as inputs, and give the outlet temperature as an output. Further details are given by Xu and Spitler (2006).

3.3 Cooling Tower Model

Two versions of a cooling tower model were used in this work. First, the fixed-*UA* cooling tower model developed by Khan (2004), determines the exiting water temperature, as well as the exiting air wet-bulb temperature based on five inputs; water mass flowrate, air mass flowrate, entering water temperature, entering air wet-bulb temperature, and a cooling tower on/off control signal. The model also requires one parameter, the overall heat transfer coefficient which is estimated from the manufactures data and set as constant. From this parameter, an effective UA value, UA_e, is calculated according to the following equation.

$$UA_e = UA\frac{C_{pe}}{C_{p,moistair}} \tag{4}$$

Where C_{pe} is the effective specific heat (J/kg-K), $C_{p,moistair}$ is the moist air specific heat (J/kg-K).

The fixed-*UA* model seemed most appropriate at the beginning of the work. For the small cooling tower used with the system, only a single operating point was available from the manufacturer. If more data were available from the manufacturer, a more detailed model would be appropriate. For the validation, one of the improvements was to utilize the parameter-estimated-*UA* model proposed by Lebrun and Silva (2002):

$$UA_e = \left[k\dot{m}_w^x \dot{m}_a^y\right]\frac{C_{pe}}{C_{p,moistair}} \tag{5}$$

3.4 Plate Frame Heat Exchanger Model

Hybrid ground source heat pump systems often use a liquid-to-liquid plate frame heat exchanger to isolate the cooling tower from the rest of the system. Initially, a parameter estimation-based model was developed, based on the general concept of Rabehl, et al. (1999). Rabehl, et al. developed a model of a fin-tube heat exchanger based on assumed correlations which were reduced to equations with a few unspecified parameters. These parameters were then fitted using catalog data. In this model, the plate frame heat exchanger is assumed to behave approximately as a series of flat plates with unknown critical local Reynolds numbers. Incropera and DeWitt (2002) give a general form as:

$$Nu_L = (0.037\,\mathrm{Re}_L^{4/5} - A)\,\mathrm{Pr}^{1/3} \tag{6}$$

Here, A is a variable that depends on the critical Reynolds number, but it may be grouped into another fitted parameter. We are interested in finding hA on both sides of the heat exchanger, and both sides have the same general form of the correlation. Assuming the length L, heat exchanger area A, cross-sectional area A_c are unknown, the equation for hA can be reduced to:

$$hA = \left(c_1 \frac{Q^{4/5}}{\nu^{4/5}} - c_2 \right) \mathrm{Pr}^{1/3}\, k_{fluid} \tag{7}$$

Where Q is the volumetric flow rate (m^3/s), ν is the viscosity (m^2/s), Pr is Prandtl number (-), k_{fluid} is the thermal conductivity of the fluid, c_1 and are c_2 constants to be fitted.

Fluid properties are determined at the film temperature on each side of the heat exchanger, and separate coefficients are fitted for each side of the heat exchanger, using manufacturer's catalog data. Furthermore, it was initially assumed that the UA may be simply determined as the inverse of the sum of the two convective resistances. The validity of this assumption will be discussed in the results section.

3.5 Cooling Tower Controller Model

Two approaches to modeling the cooling tower control have been taken. For the first set of simulations, cooling tower on/off operation is simply set as a boundary condition. For the second set of simulations, a simple model of the cooling tower controller takes the difference between the outdoor ambient wet-bulb temperature, provided as a boundary condition, and the simulated exiting heat pump fluid temperature. When the difference exceeds a specified value, e.g. 4ºC, the cooling tower is switched on. When the difference falls below another specified value, e.g. 2ºC, the cooling tower is switched off. The two approaches are discussed further in the section "System Simulation" below.

3.6 Empirical Pipe Heat Loss/Gain Model

As described above in the "Experimental Facility" section, the uninsulated piping, either exposed to the environment or buried in the ground, has some not insignificant heat losses or gains. These heat transfers vary significantly over time. For example, the heat loss from the buried pipe leading to the cooling tower will be high (say 650 watts on average for the first 10 minutes) when the cooling tower is first switched on. After, say, an hour of cooling tower run time, the heat loss may drop to 350 watts.

As buried horizontal piping is a common feature of ground source heat pump systems, it would be useful to develop a component model that predicts the heat losses or gains. However, at present, no such model is available, and another approach was taken. A simple component model was developed that took the measured heat gain or loss as an input provided as a boundary condition, and computed the outlet temperature as:

$$T_{out} = T_{in} + \frac{Q_s}{\dot{m} C_p} \tag{8}$$

Where T_{out} is the temperature of the water leaving the pipe (^{o}C), T_{in} is the temperature of the water entering the run of pipe (^{o}C), Q_s is the measured heat transfer rate (W).

This approach worked satisfactorily when the cooling tower control was treated as a boundary condition so that the simulated cooling tower on/off operation matched the experiment well. For cases where the cooling tower control was simulated, the short time variations in the empirical pipe heat losses or gains for the piping running to and from the cooling tower are no longer meaningful. Instead, a new boundary condition was developed that used the average heat gain/loss during cooling tower runtime for each component for each day. This was set as the boundary condition for every time step of the day, and maintained the heat loss or gain approximately correctly to the extent that the simulated daily cooling tower runtime matched the actual daily runtime.

4. SYSTEM SIMULATION

As mentioned previously, the system simulation was developed within the HVACSim+ environment (Clark 1985), aided by a graphical user interface (Varanasi 2002). The simulation was developed within a single superblock and five minute time steps were used. All simulations used the following boundary conditions, measured on site, except where noted:

- Outside air wet bulb temperature, determined from an aspirated dry bulb temperature measurement (on site) and a relative humidity measured at local weather station, about 1 km from the site.
- Heat pump source side load, measured on site. This forces the heat pump operation in the simulation to be the same as the experiment.
- Flow rates of water through the heat pump/GLHE and cooling tower.
- Heat transfer rates for the empirical pipe heat loss/gain model, described above.

- The plate frame heat exchanger UA was treated as a boundary condition; a separate model was used to determine the time-varying UA based on fluid flow rates and time, when fouling was included in the UA.

Besides the variations in component models and parameters that are described in the following sections, two variations of the system simulation approach were utilized:

1. For most of the simulations presented here, the cooling tower control was modeled as a boundary condition taken from the experiment. In this case, all control interactions are, in effect, treated as boundary conditions, and the primary question of interest is the degree to which heat pump entering fluid temperatures can be correctly predicted. Secondary comparisons of interest include heat transfer rates of the various components. This type of simulation was particularly useful when "debugging" the validation, as fluid temperatures at any point in the loop could be compared directly against the experimental measurements at any time.
2. For the other simulations, the cooling tower control was modeled with a controller that mimicked the actual controller. Ultimately, this is the simulation that is of interest for validation from a designer's perspective. In this case, the questions to be asked include the degree to which the energy consumption can be predicted, the cooling tower run time, and the maximum entering fluid temperature. It is expected that, at best, the cooling tower run time fraction might be reasonably well predicted over a day. It is not expected that the cooling tower start/stop times can be accurately predicted.

For the second simulation approach, one additional boundary condition is an on/off signal that indicates whether or not the cooling tower may be operated. This prevented the simulation from running the cooling tower during the heating season or during several maintenance periods when it was turned off.

The validation simulations were performed in the order given above. We started with the models and parameters that would be feasible for a designer to obtain in advance of constructing and operating the system. While keeping the cooling tower control fixed as a boundary condition, discrepancies in temperatures were addressed by improving the individual models or their parameters. Then, the simulations with the cooling tower controller explicitly modeled were performed. Starting with the final improved simulation, we worked backwards to the initial designer-feasible models and parameters, and compared the heat pump power consumption, cooling tower run time, and maximum entering fluid temperature.

5. VALIDATION – COOLING TOWER OPERATION SET WITH BOUNDARY CONDITION

In this section, validations of each component model, individually and within the system simulation, are presented. By "individually", we mean validation of the component model by itself where the input temperatures are taken from experimental data. By "within the system simulation", we mean validation of the component model where the input temperatures are computed by the system simulation, when all fluid temperatures are being solved simultaneously.

In addition, where improvements were made to the model or model parameters, they are discussed within the component model validation discussion.

5.1 GLHE

The GLHE model requires specification of a number of parameters related to the geometry and thermal properties of the fluid, grout, and surrounding ground. While there are many parameters, the results are moderately sensitive to three parameters that are challenging to estimate precisely: the undisturbed ground temperature, the effective grout thermal conductivity, and the effective ground thermal conductivity.

For larger commercial systems, these parameters are typically estimated as part of an in situ thermal conductivity test, which would be performed for one or a few test boreholes. (Austin et al. 2000, Shonder and Beck 2000, Gehlin and Nordell 2003). Additional uncertainty, beyond sensor errors, is introduced because of the nonhomogeneous nature of the ground; the time-varying nature of the undisturbed ground temperature, which is affected by seasonal changes near the surface; and downhole variations in the U-tube location and borehole diameter. Hern (2004) measured all three boreholes; the range of values and mean value are summarized in Table 1. The calibrated values are found by minimizing the sum-of-the-squares-of-the-error of the GLHE exiting fluid temperature for the seven month period evaluated here. Because the parameters are interrelated, the calibration may find best-fit values that are outside the estimated uncertainty range of the experimental measurements, as found for the effective grout thermal conductivity.

Table 1. GLHE Parameters

Parameter	Range measured by Hern (2004)	Mean measured by Hern (2004)	Estimated Uncertainty	Calibrated Value
Undisturbed ground temperature (^{o}C)	17.1-17.4	17.25	± 1.0 º C	18.0
Effective grout thermal conductivity (W/m-K)	1.07-1.09	1.08	± 15%	1.56
Effective ground thermal conductivity (W/m-K)	2.4-2.7	2.55	± 15%	2.25

Figure 4 compares experimental and simulated outlet temperatures resulting from the component GLHE simulation (calibrated and uncalibrated) as well as the system simulation (calibrated only) for five hours of a typical cooling day. Figure 5 gives the heat transfer rates for the same time period. During these five hours, the heat pump went through two on/off cycles. During the off portion of the cycle, it may be noted that there is a small negative heat transfer rate. The circulation pump was operated continuously. Also, during this time period, the cooling tower was operated continuously, and heat was exchanged between the ground and the horizontal piping that runs between the plant and the cooling tower. The net effect is the small negative heat transfer rate; i.e. heat is being extracted from the ground, and is "pre-cooling" the ground during the heat pump off cycle.

For the component simulations, the experimental inlet temperature was used to drive the model. As expected, the calibrated component model simulation with the correct inlet temperature gives the best results. It represents a small improvement over the uncalibrated component model simulation. It may be inferred from this that the thermal properties measured with the in situ test

give adequate accuracy. The system simulation, which uses the inlet temperature calculated by the simulation, shows an increased amount of error.

For the uncalibrated component model simulation, the root mean square error (RMSE) of the heat transfer rate over the seven month evaluation period is 463 W; the mean bias error (MBE) is 10 W, the simulation predicted, on average, 10 W more heat rejection than was experimentally measured. The calibrated component model simulation has a lower RMSE of 377 W, but an MBE of 320 W. This suggests that the calibration procedure might be rethought – perhaps the sum of the squares of the error criterion is not the best. Finally, when the calibrated model is run as part of the system simulation, the RMSE increases to 652 W, but the MBE drops to 62 W.

These errors should be compared to the experimental uncertainty of the heat transfer measurement. The uncertainty varies with flow rate and ΔT, but a typical value when the heat pump is operating is ±400 W. Figure 5 shows the upper and lower bounds on the experimental uncertainty. As shown, the system simulation produces some results that are just outside the bounds of experimental uncertainty.

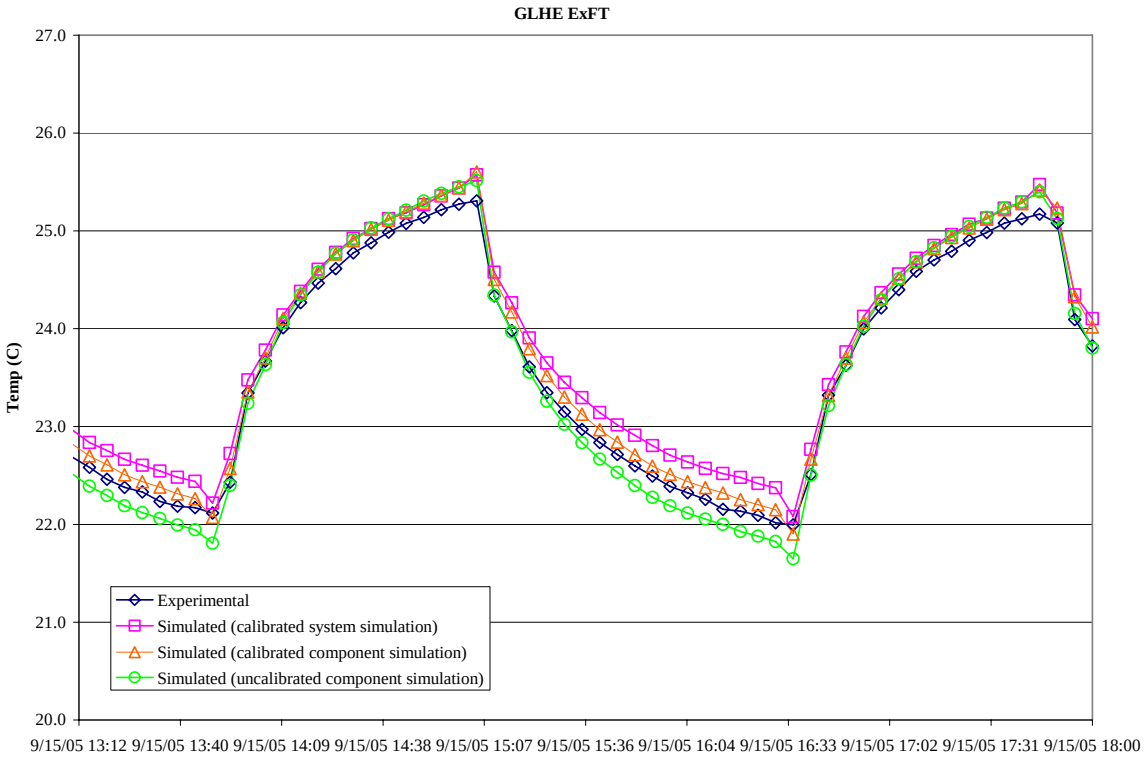

Figure 4. GLHE ExFTs for five hours of a typical cooling day

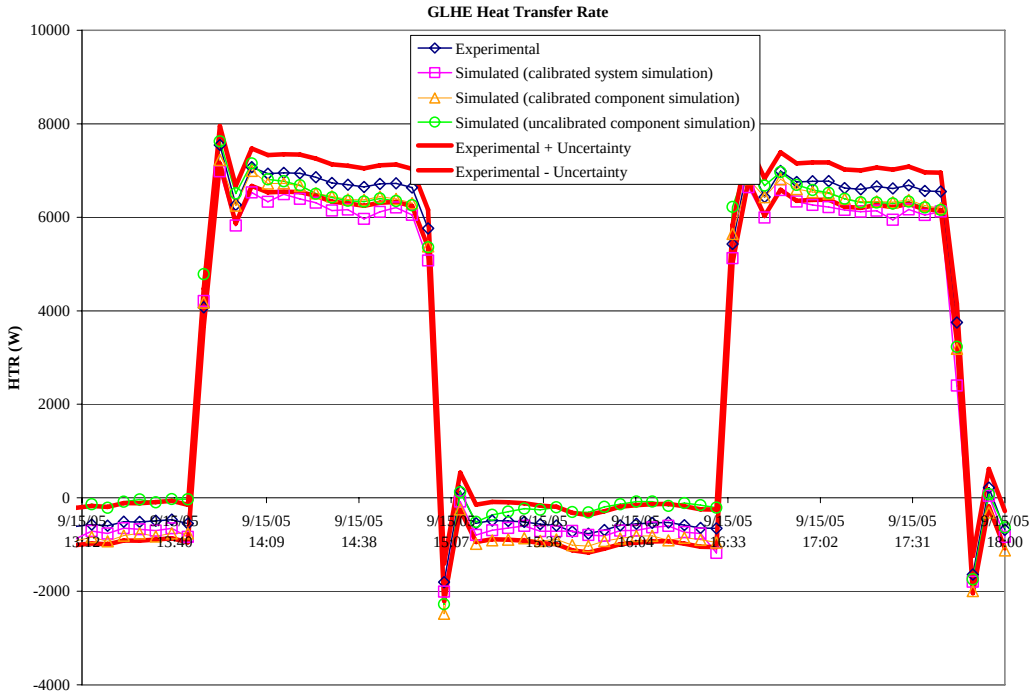

Figure 5. GLHE heat transfer (rejection) rates for five hours of a typical cooling day

5.2 Cooling Tower

As the cooling tower manufacturer gave only a single operating point as catalog data, the first cooling tower model utilized a fixed UA value of 800 W/K. For larger cooling towers, additional manufacturer's data should be available to support a variable-UA model. For our experiment, the variable UA model was developed based on measured data, resulting in:

$$UA_e = \left[764\dot{m}_w^{1.11}\dot{m}_a^{0.41}\right]\frac{C_{pe}}{C_{p,moistair}} \tag{9}$$

Figures 6 and 7 show results for a portion of a typical cooling day, with several cooling tower on/off cycles. Here, the uncalibrated component simulation represents the results from the fixed UA model; while the calibrated simulations represent results with the variable-UA model. The model improvements do not result in obviously significant improvements in the model predictions. The RMSE in the heat transfer rate is 862 W for the uncalibrated component simulation. Going to the calibrated variable UA model only reduces the RMSE to 762 W. However, the MBE goes from 329 W to 71 W of overprediction by the simulation. When the calibrated model is simulated as part of the system, the RMSE is 359 W and the MBE is 16 W of underprediction by the simulation.

The lower and upper bounds of the experimental uncertainty in the cooling tower heat transfer rate measurement are shown in Figure 7. In addition, the simulation has an experimental uncertainty component – the wet bulb temperature (an input) has a typical uncertainty of ± 0.5ºC

– and this results in an uncertainty in the simulation results. Error bars are shown for a couple sample points in Figure 7. The uncertainty caused by the uncertainty in the wet bulb temperature appears to be the limiting factor in the simulation. This also suggests that, in practice, caution is warranted in using a control based on wet bulb temperature.

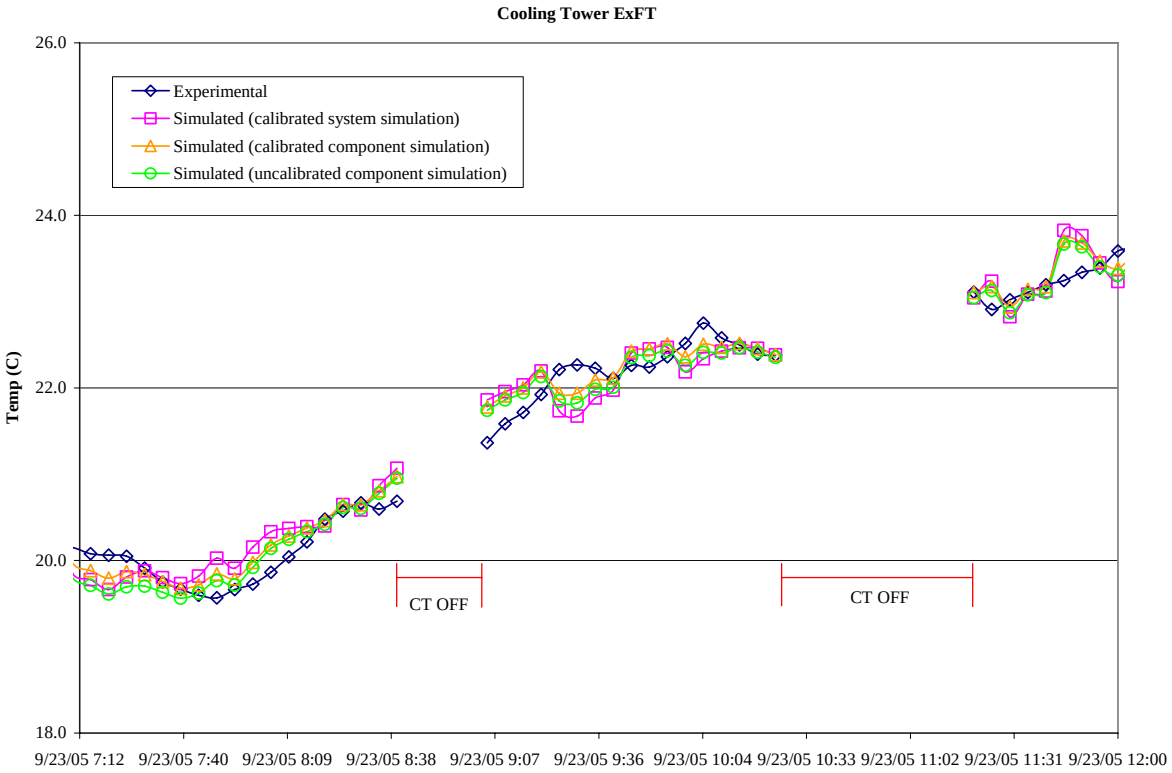

Figure 6. Cooling tower ExFTs for a typical cooling day

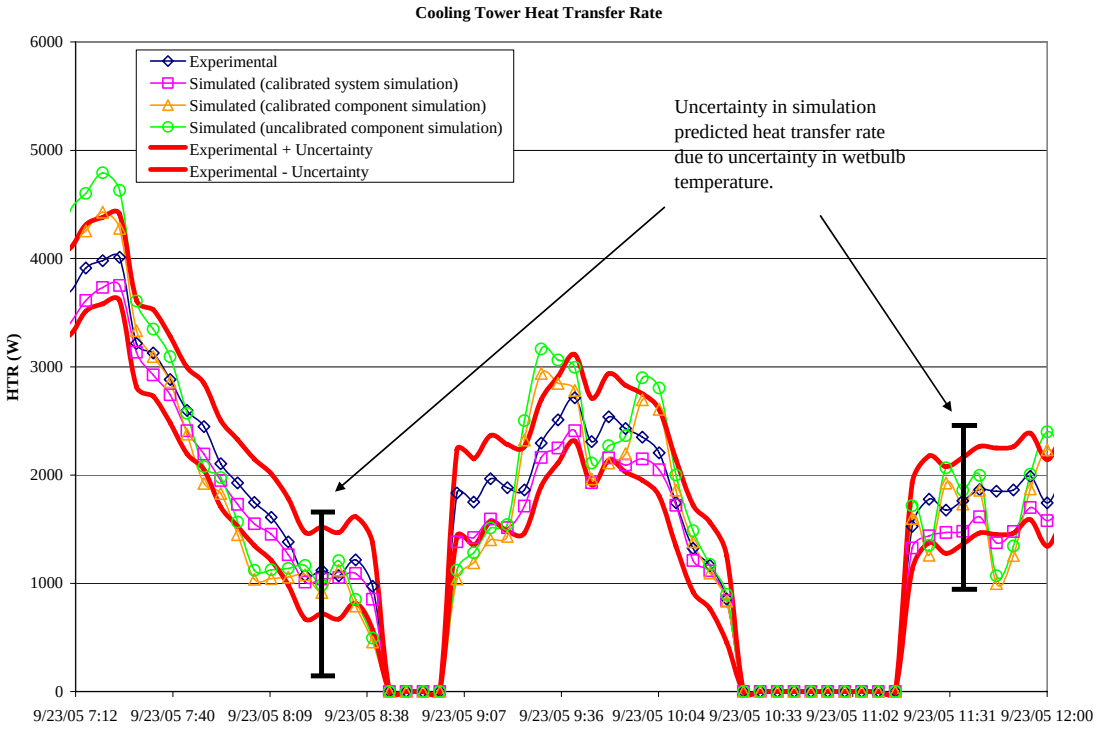

Figure 7. Cooling tower heat transfer rates for a typical cooling day

5.3 Heat Pump

Coefficients for the equation-fit heat pump model were initially calculated using manufacturer's data – the resulting model is labeled as "uncalibrated" in Figures 8-10. The model gave poor results in heating mode due to the fact that the actual flow rates on both sides of the heat pump were larger than catalog data. This may be unavoidable in equation-fit models and could perhaps be addressed by specifying flow rate and temperature limits in the component model. However, it was addressed in our case by using experimentally-measured data points in the data set and recalculating the model coefficients. Table 2 and Figures 8 and 9 show substantial improvements when this calibration is done. However, a recommendation for system designers is still needed and is a subject of future work.

Table 2 Summary of Uncertainties in HP model

Model	Source Side HTR RMSE (W)	Source Side HTR Mean Bias Error (W)	Load Side HTR RMSE (W)	Load Side HTR Mean Bias Error (W)	Power RMSE (W)	Power Mean Bias Error (W)	Source Side HTR Typical Uncertainty	Load Side HTR Typical Uncertainty	Power Typical Uncertainty
Simulated (calibrated system simulation)	451	-141	171	-33	77	-32	450 W	500 W	4.5 W
Simulated (calibrated component simulation)	457	-179	72	12	27	5			
Simulated (uncalibrated component simulation)	1823	1113	751	-333	414	-81			

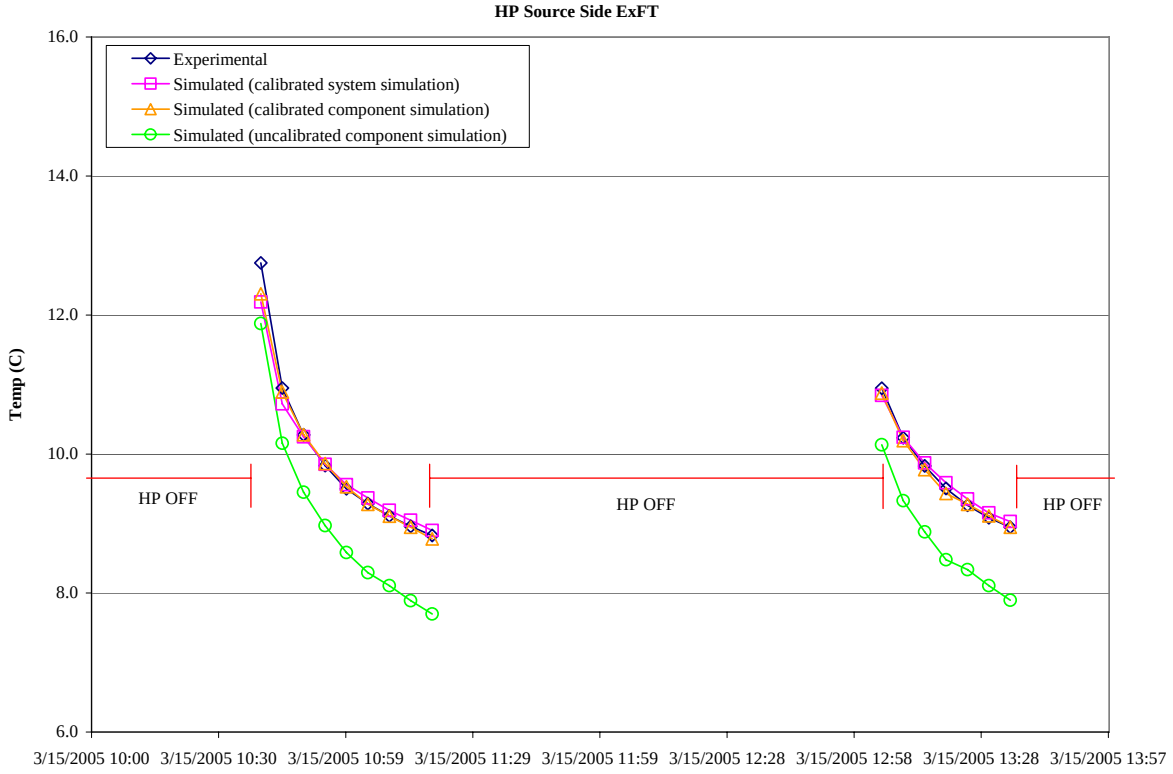

Figure 8. HP Source side ExFT for a typical heating day

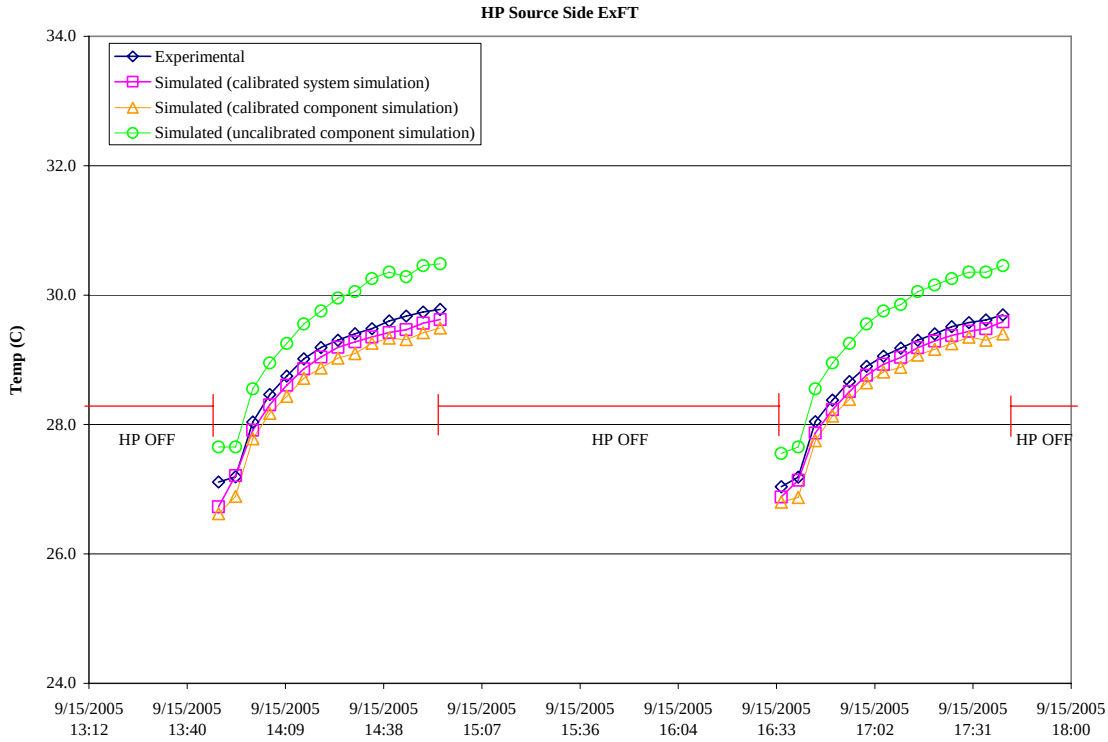

Figure 9. HP Source side ExFT for a typical cooling day

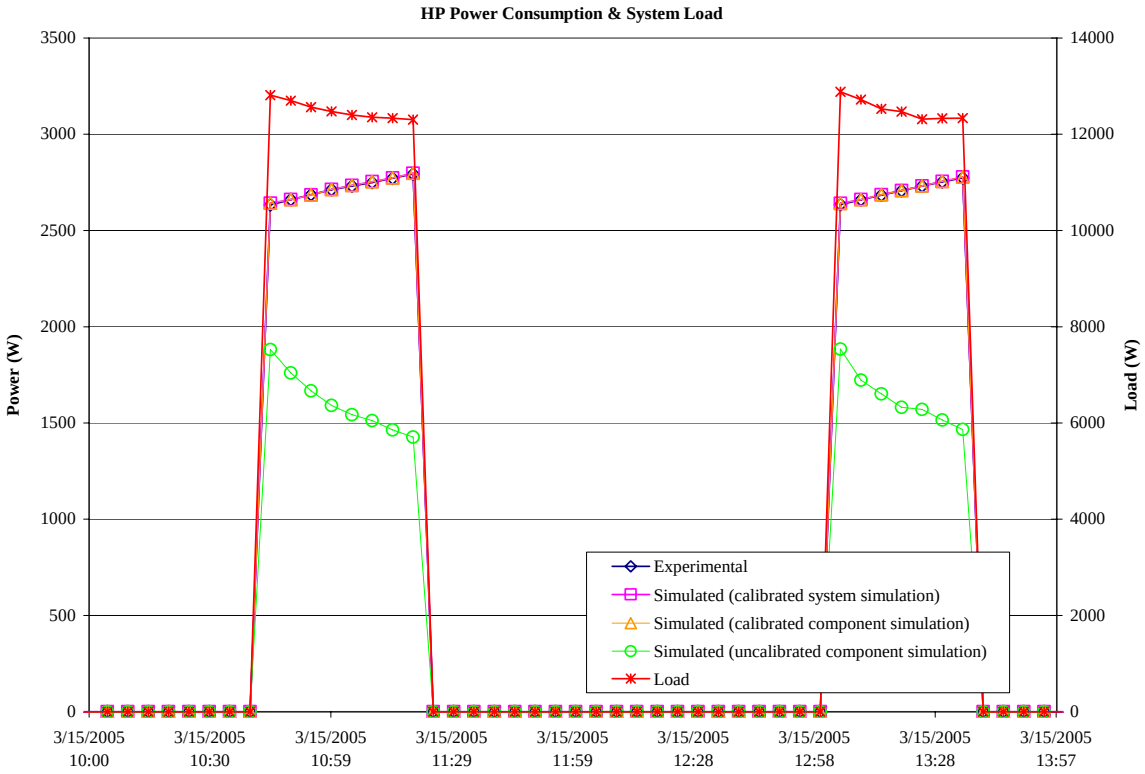

Figure 10. HP power consumption and load for a typical heating day

5.4 Plate Frame Heat Exchanger

Sixteen data points were available from the manufacturer of the plate frame heat exchanger model. Initially, a fixed UA model was utilized for the heat exchanger with a value of 800 W/K. However, calculation of the UA value at every time step based on experimental measurements revealed two interesting phenomena:

1. First, the UA varied moderately as fluid flow rates and temperatures changed. This phenomenon was addressed by developing the parameter estimation-based model, based on the general concept of Rabehl, et al. (1999), as described above.
2. More significantly, the UA decreased substantially over the seven month period of experimentation. Significant fouling was observed on the cooling tower supply of the loop, and a chemical treatment regime introduced belatedly did not reverse the UA degradation. Prediction of fouling does not seem to be feasible, so a heuristic approach was taken by adding a fouling factor that increased linearly with time.

Figure 11 shows a comparison of the various simulations with the experimental results. Clearly, the original approach, without the fouling adjustment, yields large errors. With the fouling adjustment the system simulations give heat transfer rates that are substantially improved. However, the model results are better for the typical cooling day than other days. The RMSE of the heat transfer rate prediction is 1839 W for the uncalibrated model; 854 W for the calibrated model; and 968 W for the calibrated model in the system simulation. The MBE is 1380 W of overprediction for the uncalibrated model; 311 W of overprediction for the calibrated model; and

3 W of underprediction for the calibrated model in the system simulation. So, while the calibration process helps significantly, the inherently unpredictable nature of fouling leaves a difficulty for the system designer.

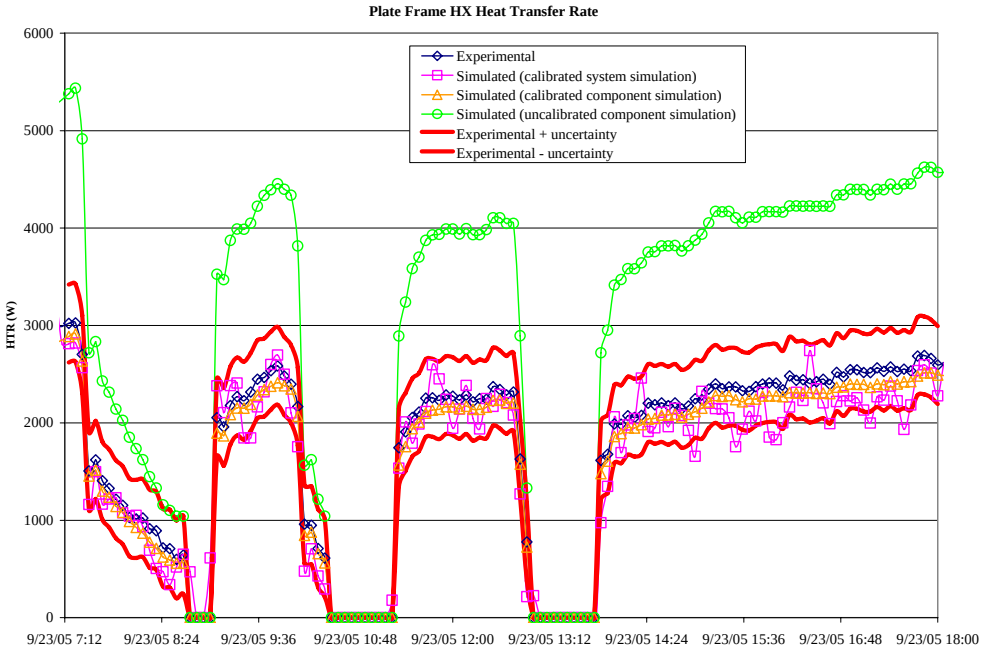

Figure 11. Plate frame HX heat transfer rate for a typical cooling day

6. VALIDATION – COOLING TOWER CONTROL SIMULATED

After adjusting component models and their parameters while setting the cooling tower operation to exactly match the experimental data, attention may be turned to the broader question of how the model performs with the cooling tower control explicitly modeled. Again, this is the simulation that is of interest for validation from a designer's perspective. In addition to looking at the final calibrated simulation, the intermediate steps between the starting case and the final calibrated simulation will also be examined. Three results are of primary interest: system energy consumption, cooling tower run time, and maximum entering fluid temperature to the heat pump.

Starting with the system energy consumption, Figure 12 shows the component-by-component energy consumption over the entire period, starting with the starting case, then showing each incremental improvement. Clearly, there is little difference in total energy consumption between any of the five model variations. Despite having improved the fidelity of the model with respect to fluid temperatures, this has made a small difference in the energy consumption, with the best model being the starting case, with no calibration. Presumably, this is coincidental, but it does provide hope that, for the designer, reasonable accuracy in predicting energy consumption can be had with information available at the time of the design. By way of explanation, energy consumption by the heat pump is the largest component of the system energy. While there is definitely a relationship between entering fluid temperature and energy consumption, a few degrees Celsius error does not make a significant difference in energy consumption.

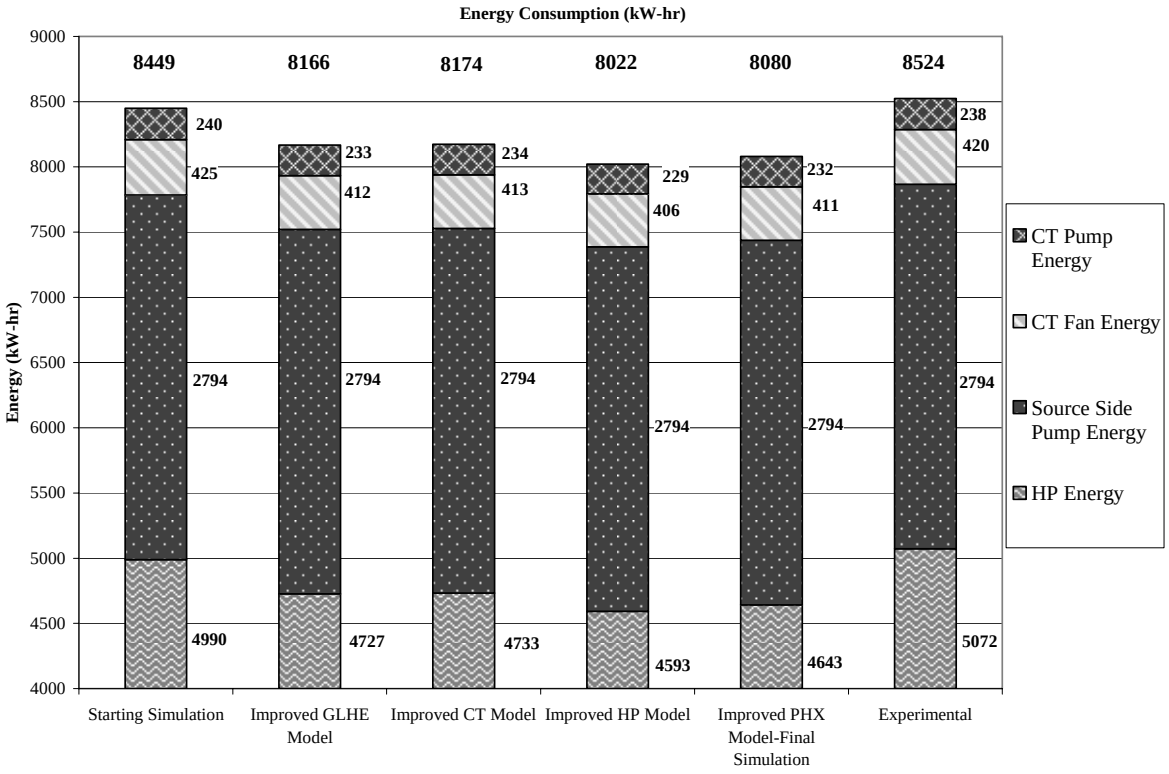

Figure 12. System energy consumption, March-September – incrementally improved simulations vs. experimental measurements. Note: Y-axis begins at 4000 kW-hr

The monthly energy consumption for the final calibrated simulation and the experiment is shown in Figure 13. With the exception of the month of June, there is quite a good match between the simulated energy consumption and the experimental measurements.

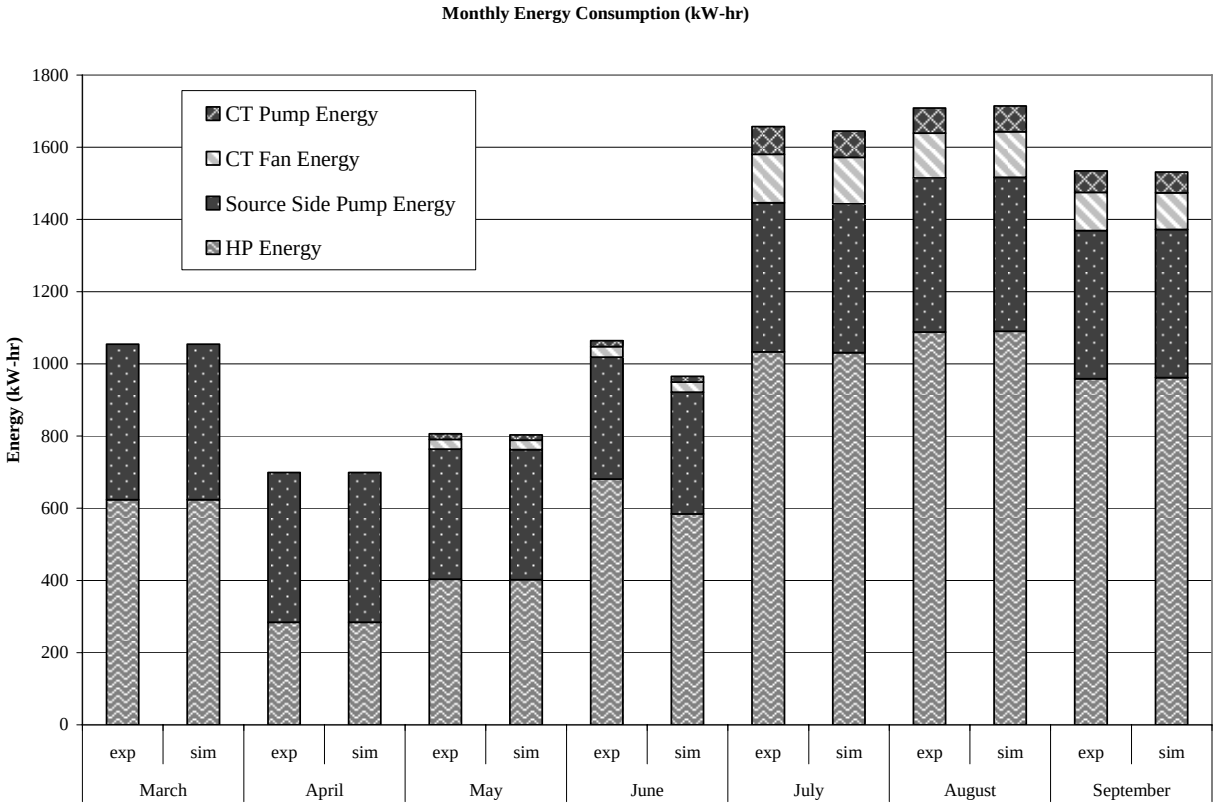

Figure 13. Experimental vs. simulated monthly energy consumption

The cooling tower run times predicted by each model variation and the experiment are summarized in Table 3. Again, all variations of the model fall within a few percent of the experimental results, and this accuracy should be quite adequate for any design simulation.

Table 3. Cooling Tower Run Times

	Starting Case	Improved GLHE Model	Improved CT Model	Improved HP Model	Improved PHX Model-Final Simulation	Experimental
Cooling Tower Run Time (Hours)	1805	1752	1754	1724	1745	1786

A final parameter of interest is the predicted maximum entering fluid temperature. Ground loop heat exchangers serving cooling-dominated buildings are generally sized to not exceed a maximum entering fluid temperature, so this parameter is of particular interest. As shown in Table 4, all of the simulations overpredict the maximum entering fluid temperature, although the model improvements generally increase the accuracy.

Table 4. Maximum heat pump entering fluid temperatures

	Starting Case	Improved GLHE Model	Improved CT Model	Improved HP Model	Improved PHX Model-Final Simulation	Experimental
Max HP EFT (^{o}C)	32.7	32.5	32.6	30.3	30.5	29. 9

6. CONCLUSIONS AND RECOMMENDATIONS

This paper describes a validation of a hybrid ground source heat pump system simulation, previously unreported in the literature. The validation was considered from two perspectives. First, it was considered from the researcher's perspective, where calibration of individual model components can be used to improve the match between simulation and experiment and provide insight into the nature of the model performance. From this perspective, the simulation is able to provide an acceptable match to the experimental results. In particular, calibration of the heat pump model gives a significant improvement in the results. Calibration of the cooling tower model and plate frame heat exchanger model give significant improvements, but limitations in the accuracy of the wet bulb temperature measurement and knowledge of fouling are obstacles to achieving further improvements.

Second, the validation was considered from the designer's or simulation user's perspective, where calibration of models based on operating data is impossible since the simulation is informing the design. From this perspective, the performance of the system simulation with all models relying only on manufacturers' data was quite good and should be acceptable for design purposes. For the seven month period of operation reported here, the uncalibrated system simulation gave total energy consumption within 1% of actual, qualified by:

- The system simulation had the advantage of perfect knowledge of the system loads and near-perfect knowledge of the weather. No designer will have these advantages!
- The goodness of the results for the uncalibrated model certainly relied on counteracting errors. This is illustrated by the succession of "incremental improvements" to the system simulation, which do not necessarily improve the accuracy. The "best" simulation with all "improvements" gives total energy consumption about 6% less than the experiment.
- The system simulation here relies on experimental measurements for heat losses and gains in buried and exposed piping. Use of models for the piping losses/gains would introduce additional error.

Recommendations for further research and development include the following:

1. As horizontally-buried piping is a common feature of GSHP systems, it would be useful to have a component model that covers this feature.
2. The equation-fit-based heat pump model used here performed poorly with catalog data. A parameter-estimation-based model and/or some checks on the input data to the model combined with some more intelligent extrapolation should be investigated.
3. The sensitivity of the cooling tower results to the uncertainty in wet bulb temperature suggests caution by practitioners when using control based on the wet bulb temperature. Further research into control strategies that either do not depend on the wet bulb temperature or that only partly depend on the wet bulb temperature is warranted.

4. While it is almost certainly impossible to predict fouling in an accurate manner, research that investigates fouling scenarios and approximate approaches may make it possible to develop recommendations for designers.

REFERENCES

ASHRAE. 1995. Commercial/Institutional Ground-Source Heat Pumps Engineering Manual. Atlanta: American Society of Heating, Refrigerating and Air-Conditioning Engineers, Inc.

Austin, W., C. Yavuzturk, J.D. Spitler. 2000. Development Of An In-Situ System For Measuring Ground Thermal Properties. *ASHRAE Transactions* 106(1):365-379.

Chiasson, A. D., C. Yavuzturk. 2003. Assessment of the Viability of Hybrid Geothermal Heat Pump Systems with Solar Thermal Collectors. *ASHRAE Transactions* 109(2):487-500.

Clark, D. R. 1985. HVACSIM+ Building Systems and Equipment Simulation Program Reference Manual. NBSIR 84-2996. National Bureau of Standards.

Eskilson, P. 1987. *Thermal Analysis of Heat Extraction Boreholes*. Doctoral Thesis. University of Lund, Department of Mathematical Physics. Lund, Sweden.

Gehlin, S., and B. Nordell. (2003). Determining undisturbed ground temperatures for thermal response test. *ASHRAE Transactions*. 109(1): 151-156

Hern, S. 2004. *Design of an Experimental Facility for Hybrid Ground Source Heat Pump Systems*. M.S. Thesis, Oklahoma State University, School of Mechanical and Aerospace Engineering. Available online at www.hvac.okstate.edu.

Incropera, F.P., and DeWitt, D.P., 2002. *Fundamentals of Heat and Mass Transfer*. 5th ed. John Wiley & Sons, Hoboken, NJ.

Kavanaugh, S.P. 1998. A design method for hybrid groundsource heat pumps. *ASHRAE Transactions* 104(2):691- 698.

Khan, M.H., A. Varanasi, J.D. Spitler, D.E. Fisher, R.D. Delahoussaye. 2003. Hybrid Ground Source Heat Pump System Simulation Using Visual Modeling Tool For Hvacsim+. Proceedings of Building Simulation 2003 pp. 641-648. Eindhoven, Netherlands.

Khan, M. 2004. Modeling, Simulation and Optimization of Ground Source Heat Pump Systems. M.S. Thesis, Oklahoma State University, School of Mechanical and Aerospace Engineering. Available online at www.hvac.okstate.edu.

Lebrun, J., and Silva, C.A. 2002. Cooling tower – model and experimental validation. *ASHRAE Transactions* 108(1):751-759.

McLain, H.A., and M. Martin. 1999. A preliminary evaluation of the DOE-2.1E ground vertical well model using Maxey School measured data. *ASHRAE Transactions* 105(2): 1233-1244.

Phetteplace, G., and W. Sullivan. 1998. Performance of a hybrid ground-coupled heat pump system. *ASHRAE Transactions* 104(1):763-770.

Rabehl, R.J., J.W. Mitchell, and W.A. Beckman. 1999. Parameter Estimation and the Use of Catalog Data in Modeling Heat Exchangers and Coils. HVAC&R Research 5(1):3-17.

Ramamoorthy, M. H. Jin, A. Chiasson, J.D. Spitler. 2001. Optimal Sizing of Hybrid Ground-Source Heat Pump Systems that use a Cooling Pond as a Supplemental Heat Rejecter – A System Simulation Approach. *ASHRAE Transactions* 107(1):26-38.

Shonder, J.A., and J. Beck. 2000. Field Test of a New Method for Determining Soil Formation Thermal Conductivity and Borehole Resistance. *ASHRAE Transactions* 106(1): 843-850.

Singh, J.B., and G. Foster. 1998. Advantages of Using the Hybrid Geothermal Option. The Second Stockholm International Geothermal Conference. The Richard Stockton College of New Jersey.

Tang, C.C. 2005. *Modeling Packaged Heat Pumps In A Quasi-Steady State Energy Simulation Program.* M.S. Thesis, Oklahoma State University, School of Mechanical and Aerospace Engineering. Available online at www.hvac.okstate.edu.

Thornton, J.W., T.P. McDowell, J.A. Shonder, P.J. Hughes, D. Pahud, and G. Hellstrom. 1997. Residential vertical geothermal heat pump system models: Calibration to data. *ASHRAE Transactions* 103 (2): 660-674.

Varanasi, A. 2002. Visual Modeling Tool for HVACSIM+. M.S. Thesis, Oklahoma State University, School of Mechanical and Aerospace Engineering. Available online at www.hvac.okstate.edu.

Xu, X., J. D. Spitler. 2006. Modeling of Vertical Ground Loop Heat Exchangers with Variable Convective Resistance and Thermal Mass of the Fluid. Proceedings of the 10th International Conference on Thermal Energy Storage. Ecostock 2006, Pomona, NJ.

Yavuzturk, C., J.D. Spitler. 1999. A Short Time Step Response Factor Model for Vertical Ground Loop Heat Exchangers. *ASHRAE Transactions* 105(2): 475-485.

Yavuzturk, C., J.D. Spitler. 2000. Comparative Study to Investigate Operating and control Strategies for Hybrid Ground Source Heat Pump Systems Using a Short Time-step Simulation Model. *ASHRAE Transactions* 106(2):192-209.

Yavuzturk, C. and J.D. Spitler. 2001. Field Validation of a short time step model for vertical ground-loop heat exchangers. *ASHRAE Transactions* 107(1): 618-626.